RD42 Internal Note 12.2

Pion Irradiation Studies of CVD Diamond Detectors

PRELIMINARY

The RD42 Collaboration

March 1, 2000

Abstract

In the vertex region of future high luminosity experiments such as LHC, detectors and frontend electronics will suffer from radiation damage. Diamond material has the reputation to be more resistive against radiation than silicon and can be used as a tracking detector instead. In the past years, various CVD diamond detectors have been irradiated with pions at the Paul Scherrer Institute (CH) and periodically characterized using a β^- source . The development of the signal output and the beam induced current vs. fluence will be discussed.

List of participants

Experimental Realization and Analysis:

W.Adam (wolfgang.adam@cern.ch)
T.Bergauer (thomas.bergauer@oeaw.ac.at)
M.Friedl (markus.friedl@cern.ch)
J.Hrubec (josef.hrubec@cern.ch)
M.Krammer (manfred.krammer@cern.ch)
H.Pernegger (heinz.pernegger@cern.ch)
M.Pernicka (pernicka@qhepm1.oeaw.ac.at)
R.Wedenig (rudolf.wedenig@cern.ch)

Authors:

M.Friedl
J.Hrubec
M.Krammer
R.Wedenig

1 Introduction

CVD diamond allows particle detection similar to silicon. Diamond has a higher band gap of $5.5\,eV$ and therefore is electrically insulating, the dark current of detector samples is in the order of pA. Thus, a detector is simply made of a diamond film provided with ohmic contacts on opposite sides. As the charge carrier mobilities are high, the signal collection takes less than $1\,ns$, which is several times faster than in silicon. Diamond, in contrast to silicon, also withstands more radiation. One of the aims of the CERN RD42 collaboration [1] is to examine the radiation hardness of diamond detectors against pions. The results of these investigations will be described in this paper.

Tab. 1 lists the dates of the five irradiation experiments performed at the Paul Scherrer Institute (PSI) in Villigen (Switzerland) in the past years. The diamond samples were irradiated up to $1.9 \times 10^{15}\,\pi cm^{-2}$ using π^+ with a momentum of $300\,MeV/c$ and were periodically characterized.

Irradiation Experiments Overview		
Number	Date	Max. sample fluence $[10^{13}\pi cm^{-2}]$
1	06/1994	8
2	09/1995	52
3	09/1996	117
4	11/1997	110
5	09/1999	103

Table 1: Dates and maximum sample fluence of the irradiation experiments performed at the PSI.

2 Signal Generation in CVD Diamond

In contrast to silicon, CVD diamond is a poly-crystalline material. Grain boundaries may be responsible for charge trapping and recombination. Thus, only a fraction of the charge produced in the bulk by a traversing particle can be collected at the electrodes.

As a parameter to describe the mean signal output of a diamond detector, the *charge collection distance* (d_c) has been introduced. It states the mean distance an electron-hole pair drifts apart in the applied electric field before being trapped or recombining.

When CVD diamond is grown on a substrate, the grain size increases with thickness [7], which leads to better local material quality towards the growth side, i.e., more single-crystal-like diamond. This led to a model describing the local charge collection distance as a linear function of the thickness [9]. Thus thicker diamond films yield more signal. On the other hand, detectors in the vertex region should affect to a minimum the track and energy of the particles monitored. For this reason, the material must be kept as thin as possible. An optimum must be found between these criteria.

In order to get thin diamond films without losing the high quality of the growth side, material is removed from the substrate side. This technique is known as *lapping*. All the diamond samples used in the irradiation with an initial charge collection distance above $100\,\mu m$ were processed this way.

The performance of a diamond detector is characterized by the number of electrons collected at the electrodes after a minimum ionizing particle (mip) traversed the film vertically. Initially, the charge Q_p is produced by ionization per unit lenght along the particle track. Earlier work [7] reports a mean number of

$$q_p = 36e^-/\mu m \quad . \tag{1}$$

The total number of charges generated in a detector with a thickness D is $Q_{gen} = q_p D$. In the electric field applied, electrons and holes move to opposite electrodes. Due to trapping and recombination, the charge carriers in most cases do not reach the electrodes. Thus the charge collected at the electrodes (Q_c) is only a fraction of the charge produced in the bulk. We define the charge collection distance (d_c) as described above by

$$d_c = \frac{Q_c}{Q_{gen}} D = \frac{Q_c}{36} \frac{\mu m}{e^-} \quad . \tag{2}$$

The equation 2 is an appoximation for $d \gg d_c$, because surface limits are neglected. Even if this condition is violated, it is common to implicitly define the charge collection distance as stated in equation 2.

The charge collection distance depends on the material purity. Various parameters in the CVD growth process have an influence on the diamond quality. In the past years, the charge collection distance has been improved significantly by refining the manufacturer's growth process. Samples with a charge collection distance of $250\,\mu m$ corresponding to a mean signal of $9000\,e^-$ are available.

3 Samples and Setup

3.1 Samples

Tab. 2 lists the samples used for the pion irradiation.

Sample Overview			
Name	Thickness $[\mu m]$	Pad area $[cm^2]$	Total fluence $[10^{13}\pi cm^{-2}]$
TD1038-U3	447	0.196	181.1
TD1038-U4	430	0.071	67.5
DBDS43-P1	737	0.071	142.3
DBDS43-P2	760	0.071	189.8
DBDS73-R1	603	0.030	103.3
DBDS73-R2	611	0.030	105.5
DBDS74-P1	611	0.071	109.6
DBDS74-P2	641	0.071	103.5
DBDS68-Tracker	520	-	84.6
CDS71-P1	515	0.083	101.7
CDS71-P2	515	0.083	103.3
CDS71-P4	515	0.083	34.2

Table 2: The diamond samples.

All CVD diamond film samples were about half a millimeter thick. Except DBDS-68 we always had two or three samples cut from the same wafer, which behave similarly. The shape of the cut samples was usually rectangular with a circular ohmic contact well fitting on the sample on both sides. Only the samples 71p1, 71p2 and 71p4 had guard rings. The metallization was done with Cr/Au except for DBDS43-P2, which had Ti/Au contacts. No difference could be observed concerning the metallization. All contacts are ohmic. DBDS68 was a tracker and therefore metallized with strips and a square pad in one corner, which was used for the irradiation experiments. For irradiation and characterization, the contact pads were always centered in the beam spot and under the source collimator, respectively.

3.2 Irradiation Setup

The PSI runs a synchrotron accelerating protons. The spill cycle is $50\,MHz$, yielding an almost continous stream of particles. The πE1 beamline behind target E was constructed to achieve a high pion flux. In our experiments it was set up to deliver π^+ at a momentum of 300 MeV/c (correspondig to a kinetic energy of T=191 MeV) with a flux of up to $2.5 \times 10^9\ \pi cm^{-2}s^{-1}$. This value has been chosen because the cross-section of pions with ^{6}C has a maximum for π^+ at the given momentum. Secondly, the the predominant source of radiation damage in the LHC vertex region is charged pions with a momentum in the order of $300\,MeV$ [2].

Fig. 1 shows the irradiation setup. A polyethylene shield with a thickness of $3cm$ at the end of the beam line was used to reduce the proton contamination to the order of below 1%. Each diamond sample was mounted onto a Al_2O_3 sample holder with the contact pad centered over a hole to minimize the amount of material in the particle track. One or more samples were put into the beam in a slide tray, which was mounted on an xyz table. The samples were always centered in the beam spot and arranged around the beam focus. The pion beam cross-section was measured both with photopaper and using a wirechamber. Across the lateral dimension of the diamond samples, the flux inhomogenity was negligible. A light-tight cardboard box covered the tray during the whole irradiation.

On the back side of each sample holder, in the same place as the diamond sample was mounted, a $5 \times 5\,mm$ Al foil was fixed to determine the pion dose. ^{27}Al atoms are converted by pions to ^{24}Na with a half-life of 15 hours. This restricts the maximum length of a irradiation periode to 20 hours. After each period, the Al foils were put into a spectrometer to measure the amount of ^{24}Na produced. With irradiation and cooling times and the foil mass given, the received fluence can be calculated. The error of this method is estimated to be 15 %.

The proton current onto the target was measured in minute-intervals throughout the irradiation. This data was used to refine the dosimetry calculation. An ionization chamber was installed after the polyethylene shield in order to cross-check the pion fluences.

In the earlier irradiation the diamond samples were biased with $300\,V$ DC during irradiation and the pion induced current of each detector was measured individually, using a Keihtley 237 source measure unit. In the most recent irradiation the samples were biased with 500 V, which corresponds to the bias voltage used during the characterization. There was no cooling device installed; the sample temperature was about $25^\circ\,C$ throughout the irradiation.

3.3 Setup for the Characterization

Periodically, the samples were characterised, i.e., the charge collection distance was measured using a collimated $1\,mCi$ ^{90}Sr β^- source, which delivers close to minimum ionizing electrons. The characterization schematics can be seen in Fig. 2. The diamond samples were biased with DC voltages from $100\,V$ up to $800\,V$. The maximum voltage was determined by the sample thickness and choosen to correspond to an electrical field of 1V/μ m. A silicon diode beneath the diamond sample, connected to a fast amplifier, was used to trigger the readout. The diamond sample

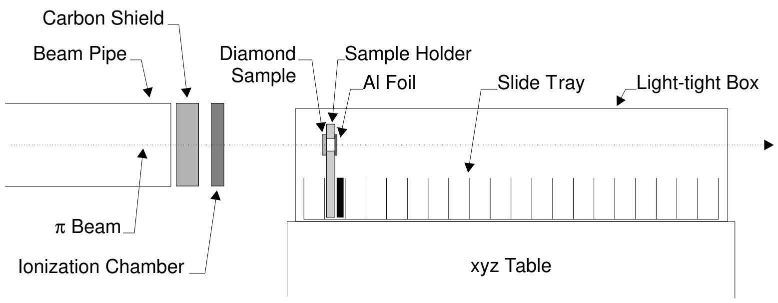

Figure 1: The irradiation setup.

was connected to a single channel of a VA2 chip[1], and the output was sent to a CAMAC unit containing an AD773 ADC. This converter is designed to take 20 MS/s, and basically sacrifices differential linearity for speed. The effect of this nonlinearity are inequal histogram binnings, causing spikes in approximately every 8th bin (fig. 3). The CAMAC crate, also containing a high voltage supply and another control module, was connected to a Macintosh computer for data recording.

The characterization station was calibrated by transmitting a small step pulse over a $3.3\,pF$ capacity into the VA2 input and by characterizing a 365 μm thick silicon diode. Using the equation of a capacitor ($Q = CV$), one can correlate ADC counts to a certain number of electrons.

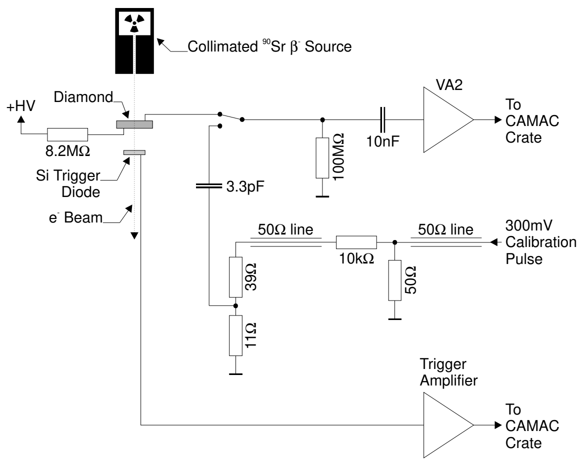

Figure 2: The characterization station.

4 Data Processing

The output of the characterization station is a pulse height spectrum of the diamond signal, which usually contains a small pedestal contribution. Fig. 3 shows two typical histograms, where the charge is given in ADC counts. The right figure shows a diamond sample with high charge collection distance, while the one to the left is a poor quality sample, where the pedestal is not separated from the signal. Secondly, when the diamond samples were measured between the irradiation periods, the samples itself and the sample holders had been activated by the pion

[1] The VA2 is a lower noise redesign of the original VIKING chip [3].

beam, causing a lot of false triggers and thus much higher pedestal contribution than normally.

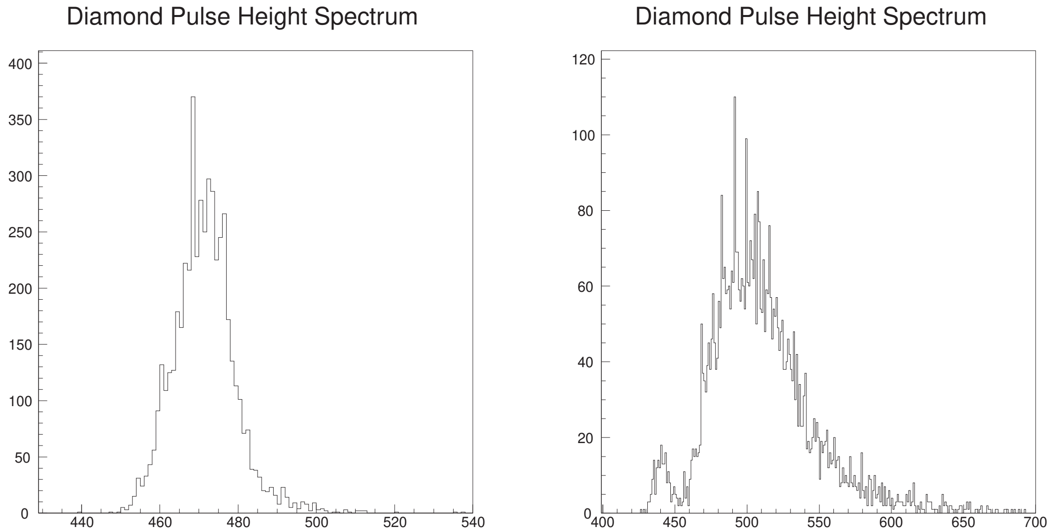

Figure 3: Typical diamond pulse height spectra. The histogram to the right shows a high d_c sample, where pedestal and signal are clearly separated, which is not the case in the left histogram of a low d_c diamond.

A fit model has been developed in order to calculate the mean signal despite the pedestal contamination. Assuming the diamond to be homogenous (which is inaccurate) and neglecting noise, we expect a Landau distributed histogram (as in silicon) plus a δ-distribution for the pedestal contribution. By adding white noise, i.e., convoluting a Gaussian Normal Distribution (see fig. 4), we obtain

$$\mathcal{H} = [\delta(pedestal) + \mathcal{L}(signal)] * \mathcal{G}(\sigma) = \mathcal{G}(pedestal, \sigma) + \mathcal{L}(signal) * \mathcal{G}(\sigma) \quad . \tag{3}$$

Considering the inhomogenous detector material, we decided to convolute the Landau part with

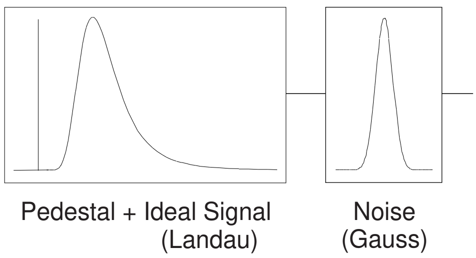

Figure 4: A model for fitting histograms.

a $\sigma_{\mathcal{L}} > \sigma$ in order to fit the measured histograms more closely.

$$\mathcal{H} = \underbrace{\mathcal{G}(pedestal, \sigma)}_{\text{pedestal}} + \underbrace{\mathcal{L}(signal) * \mathcal{G}(\sigma_{\mathcal{L}})}_{\text{signal}} \tag{4}$$

Since the fit model is a linear addition of Gaussian Normal and Landau Distributions we can easily calculate the mean of the latter when histogram and pedestal means and weights are given. Once we have calculated the Landau mean, we obtain the charge collection distance by multipling it with the calibration constant (C_{cal}).

$$d_c = C_{cal}\left(1 + \frac{\text{area}(\mathsf{pedestal})}{\text{area}(\mathsf{signal})}\right)(\text{mean}(\mathcal{H}) - \text{mean}(\mathsf{pedestal})) \tag{5}$$

For diamonds with reasonable pedestal separation, it is much easier to calculate the charge collection distance, simply cutting out the pedestal contribution. This way has been cross-checked by other methods, yielding similar results.

Three components contribute to the error of the charge collection distance measurements. First, the calibration uncertainty is estimated to be approximately 10% due to unknown stray capacitance. Secondly, the preamplifier's noise with the detector connected is in the order of 300 electrons, or $8\mu m$ of charge collection distance, which is deduced from pedestal measurements. Finally, statistic fluctuations of the pulse height spectra and the bad separation of pedestal and signal contributions lead to a uncertainty in the fitting procedure of approximately 10%. Thus, the total error of the charge collection distance is estimated to be about 14%.

5 Results

For the operation of tracking detectors, a reasonable signal-to-noise ratio (SNR) is essential. Two components are mainly responsible for this figure, the detector and the preamplifier. With common readout systems, the signal is determined by the detector only, while the noise depends on the preamplifier and the detector capacity. In this context, the most important figure of diamond is the signal output, which is presently in the order of several thousand electrons. In the past years, the quality of the diamond samples has been dramatically improved by refining the manufacturer's growth process.

5.1 Pumping Effect

The signal output of diamond can by increased by low dose ionizing radiation. This effect saturates at an empirical value of about 1.6 times the initial signal height at approximately $10^{10}\,\pi cm^{-2}$. Diamond converted to this *pumped state* can be reset to the original (or, *depumped state*) by exposure to ultra violet light. This process is fully reversible [4, 5, 6]. In the pion beam, the pumping process can be monitored as an increase of the beam induced current, as shown in Fig. 5. At zero fluence, the beam shutter opens, causing a steep rise. After that, the increase in the current due to the pumping effect is clearly visible.

During irradiation, trapping centers in the diamond are filled by the ionization of crossing particles, allowing the electrons and holes to move farther and thus increasing the output signal. The trapping centers can be discharged by UV light [Ref. weiss noch nicht welche].

As the diamond samples, exposed to the pion beam at a flux of typically $2 \times 10^{9}\,\pi cm^{-2}s^{-1}$ reach the pumped state within seconds, we always refer to the pumped state values. This will also be the working condition in future experiments.

5.2 Charge collection distance

Tab. 3 lists the charge collection distances before and after irradiation measured in the pumped state at $1\,V/\mu m$ by four different groups (Vienna, CERN, Ohio, Nikhef). The pulse height distribution of sample 71p1 before and after irradiation is shown in Fig 6 (left). The mean signal decreases by 51 %, the most probable by 41 %. The pulse height distribution gets narrower after

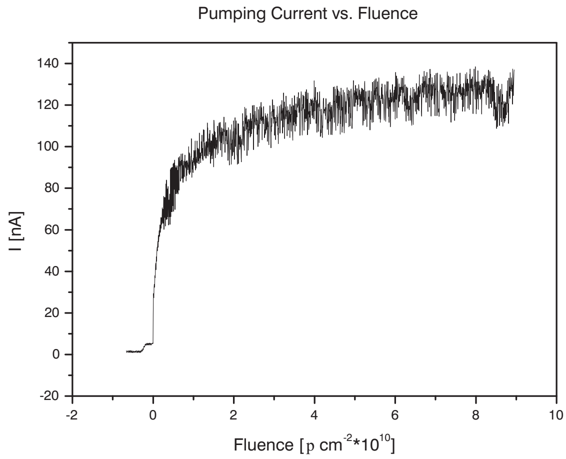

Figure 5: The pion beam induced current during pumping.

irradiation and is shifted towards lower values. But there is still a clear separation between the pedestal and the signal itself, which is relevant for detector applications with a given threshold (i.e the ATLAS and CMS pixel readout chips), because the detector will not lose efficiency.

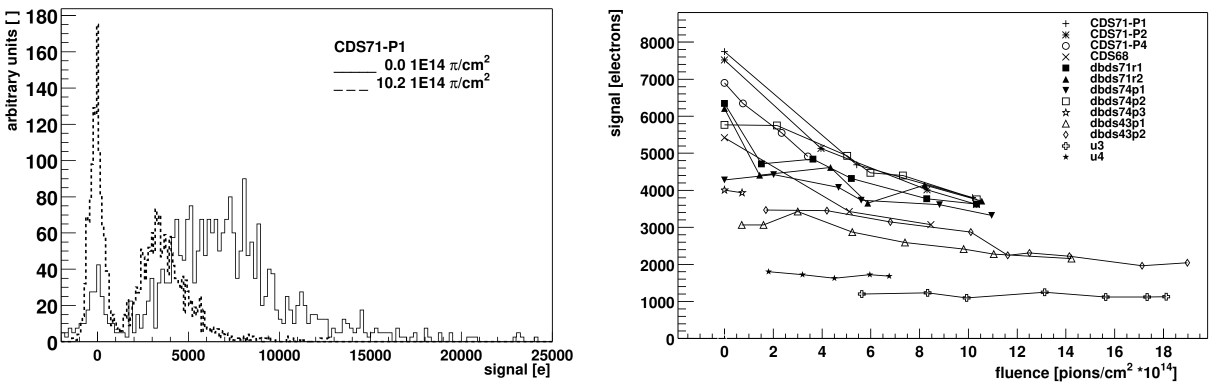

Figure 6: Pulse height distribution of sample 71p1 before irradiation and after it accumulated $1.2 \times 10^{15} \pi/cm^2$ (left). Charge collection distances vs. fluence (right).

In Fig. 6 (right) the charge collection distance vs. fluence is shown for all samples measured by the Vienna group. We find the higher the charge collection distance is initially, the faster it drops. This effect could be explained by the linear model of the charge collection distance. The vertical trap density across the detector before irradiation is higher at the substrate side than on the growth side. Thus the local charge collection distance is low on the substrate side and high at the growth side. Heavy irradiation is expected to introduce additional traps, equally distributed along the particle track. The sum trap density now increases significantly on the subtrate side, shrinking the local charge collection distance significantly, while there is only a negligible relative rise at the growth side. In other words, regions with a high charge collection distance are more susceptible to radiation damage than those with low d_c, which are relatively indifferent.

Fig. 7 shows the charge collection distance normalized to its unirradiated value vs. fluence for samples of comparable and high quality (ccd $\approx 200\mu$m). As fit function we used the equation,

Charge collection distances					
Name	Total fluence $[10^{14} \pi cm^{-2}]$	Q_{ccd} Vienna $[e^-]$	Q_{ccd} CERN $[e^-]$	Q_{ccd} Ohio $[e^-]$	Q_{ccd} Nikhef $[e^-]$
TD1038-U3	0	-	-	1692	-
	18.1	1116	1764	?	-
TD1038-U4	0	-	-	1764	-
	6.8	1764	1728	?	-
DBDS43-P1	0	3060	3708	2808	-
	14.2	2160	2196	?	-
DBDS43-P2	0	-	3240	3384	-
	19.0	2052	2196	?	-
DBDS73-R1	0	6336	6084	?	-
	10.3	3636	3744	?	-
DBDS73-R2	0	6228	6588	?	-
	10.6	3708	3240	?	-
DBDS74-P1	0	4284	4788	?	-
	11.0	3312	3420	?	-
DBDS74-P2	0	5760	6488	?	-
	10.4	3744	4248	?	-
DBDS68-Tracker	0	5400	-	-	-
	8.5	3050	-	-	-
CDS71-P1	0	7750	-	6150	-
	10.2	3800	-	-	3730
CDS71-P2	0	7500	-	6231	-
	10.3	3600	-	-	3750
CDS71-P4	0	6900	-	-	-
	3.4	4900	-	-	4800

Table 3: The charge collection distances before and after irradiation.

$$\sigma = \sigma_0 \frac{1}{1 + \alpha f}, \tag{6}$$

with σ_0, the signal of the unirradiated sample, σ, the signal at the fluence f and α, the damage constant. Eq. 6 is derived from the hypothesis that the signal scales with the inverse number of traps n

$$\sigma \propto \frac{1}{n} = \frac{1}{n_0 + n_i}, \tag{7}$$

with n_0, the initial number of traps, and n_i, the number of traps created by irradiation. Substituting $\sigma_0 = 1/n_0$ and $n_i = \alpha f$ into Eq. 7 leads to the fit function.

Our measurements show that the signal decrease of the samples with the highest charge collection distance is about 50% after $10^{15}\ \pi cm^{-2}$. This value corresponds to the estimated dose at LHC at a radius of 10 cm from the vertex within 10 years of operation [9].

5.3 Pion Beam Induced Charge

The ionization process of $300\,MeV/c$ pions crossing the diamond is very similar to that of the electrons from the β^- source, because pions with this momentum are almost mips. The basic

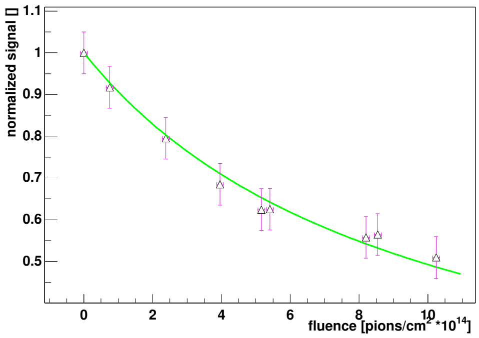

Figure 7: Normalized ccd vs. fluence

difference between the two measurements is the flux and the integration time. While during the characterization, the signal of single electrons is measured with an integration time of about 2 μs, the high pion flux allows only DC current measurements.

The beam induced current of each sample was monitored individually throughout the irradiation. Fig. 8 shows the pion induced charge for one sample. The two irradiation experiments

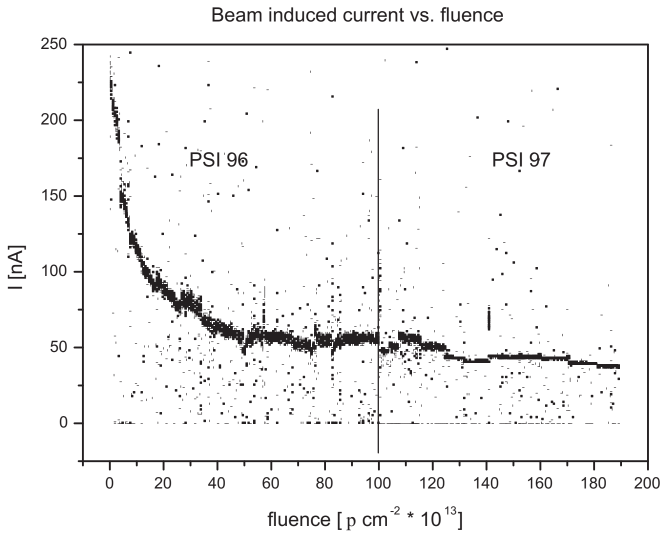

Figure 8: Pion induced current vs. fluence.

werde performed with approximately one year interval (Table 1). All samples feature a strong current decrease at the beginning of the irradiation and conserve their state over the periode between the irradiation, letting the pion induced current continue at the last periode's value. Similar results were found in neutron irradiations.

6 Summary

It has been shown that diamond detectors with sufficient signal output will survive ten years of LHC operation at a radius of $10\,cm$ from the vertex with a signal degradation of about 50%.

The charge collection distance has been improved dramatically over the past few years (up to: $250\,\mu$m or $9000\,e^-$), allowing the operation of strip and pixel detectors with reasonable SNR for tracking purposes.

Further we developed a model, based on the assumption that the signal scales with the inverse number of traps and that diamonds are also pumped by pions.

Acknowledgement

We acknowledge the help of C. Sulowski, who developed software tools for histogram manipulation and fitting [8], and the assistance of K. Gabathuler at the PSI.

References

[1] RD42 Proposal, *Development of Diamond Tracking Detectors for High Luminosity Experiments at the LHC*, CERN, DRDC 94-21, DRDC/P56, May 1994

[2] *CMS Tracker TDR 5*, CMS Collaboration, CERN/LHCC 98-6 (1998)

[3] O. Toker *et al.*, *VIKING, a CMOS Low Noise Monolithic 128 Channel Frontend For Si-Strip Detector Readout*, NIM A 340(1994), 572-579

[4] M.H. Nazaré *et al.*, *Development of Diamond Tracking Detectors for High Luminosity Experiments at the LHC*, CERN/DRDC 94-21, DRDC-P56, May 1994

[5] S. Han *et al.*, *Recent Results on the Radiation Hardness of CVD Diamond Detectors*, in the Proceedings of DPF94, Santa Fe, NM, July 1994

[6] H. Pernegger *et al.*, *Radiation Hardness Studies of CVD Diamond Detectors*, NIM A 367(1995), 207-211

[7] S. Zhao, *Characterization of the Electrical Properties of Polycristalline Diamond Films*, Ph.D. thesis, The Ohio State University, 1994

[8] C. Sulowski, *SULMAC – a Collection of PAW Macros for the Analysis of Histogramed Data*, HEPHY-PUB 665-97, March 1997

[9] M. Mishina, *Induced Charge in Diamond*, RD42 Internal Note 13, March 1998